International Journal of Computer Vision 64(1), 69–88, 2005

Wireframe Projections: Physical Realisability of Curved Objects and Unambiguous Reconstruction of Simple Polyhedra

MARTIN C. COOPER
IRIT, University of Toulouse III, 118 route de Narbonne, 31062 Toulouse, France
cooper@irit.fr

Received June 22, 2004; Revised February 3, 2005; Accepted February 14, 2005

First online version published in April 2005

Abstract. The reconstruction of an object from a single 2D projection of a 3D wireframe model is a vision problem with applications in CAD/CAM and computer graphics. We propose an algorithm for the interpretation of wireframe projections based on assigning semantic and numerical depth labels to lines. This method allows us to state necessary and sufficient conditions for the physical realisability of a wireframe projection of a curved object. The presence of linear features provides further constraints on the positions of object vertices. For example, each straight line gives rise to a coplanarity constraint between a set of object vertices.

We show that extra information, such as vanishing points, parallel lines or user-entered depth-parity information, is sufficient to uniquely determine the face-circuits in wireframe projections of polyhedra with simple trihedral vertices. In fact, a polyhedron with simple trihedral vertices can be unambiguously reconstructed from its 3D wireframe model.

Keywords: wireframe model, hidden-line drawing, physical realisability, impossible object, Necker cube, Penrose triangle

1. Introduction

The interpretation of line drawings of opaque objects is a classic problem in computer vision. Necessary and sufficient conditions have been given for the physical realisability of line drawings of polyhedral objects (Sugihara, 1986) and for curved objects with C^3 surfaces (Cooper, 1999). The computational complexity of testing the realisability of a line drawing has also been extensively studied. Although the most general problem is NP-complete (Kirousis and Papadimitriou, 1988; Cooper, 1999, 2001), the problem is solvable in linear time under certain restrictions on the drawings (knowledge of all vanishing points (Parodi and Torre, 1994; Cooper, 1999), absence of straight lines (Cooper, 1997, 1999) or possibility of contrast failure between parallel surfaces (Cooper, 2001)).

In a line drawing of opaque objects, only visible lines are shown. This is appropriate for traditional vision applications. However, for the reconstruction of the 3D shape of a human-entered object-model, a more appropriate input is a line drawing in which both visible and hidden lines are shown. Let the depth of a 3D edge E denote the number of surfaces lying between E and the viewpoint. Visible lines represent edges of depth zero. Sugihara (1986) and Alevizos (1991) have studied the interpretation of line drawings in which solid lines represent edges of even depth and broken lines represent edges of odd depth. A *wireframe projection* is a projection of all 3D edges (visible or not) in which no information concerning the depth of lines is explicitly given. When extra information is provided in the form of the 3D coordinates of each object vertex we call this a 3D *wireframe model*. The reconstruction of an

object from several wireframe projections has been extensively studied (Kuo, 1998; Wesley and Markowsky, 1981) as has the problem of converting a 3D wireframe model into a surface-based 3D model (Agarwal and Waggenspack, 1992; Jain, 1999; Leclerc and Fischler, 1992; Lipson and Shpitalni, 1996; Markowsky and Wesley, 1980; Shpitalni and Lipson, 1996; Vosniakos, 1997, 1998). Although the reconstruction of a 3D object from a user-entered wireframe is the most studied problem, other interesting applications exist, such as the indexing of technical line drawing databases (Syeda-Mahmood, 1999).

In this paper we study the interpretation of wireframe projections. We give necessary and sufficient conditions for the physical realisability of a wireframe projection when no depth information is given (in terms of depth of lines or 3D coordinates of vertices). These necessary and sufficient conditions involve not only semantic labels (convex, concave, occluding, extremal), first introduced by Huffmann (1971) and Clowes (1971) and generalised to wireframe projections by Sugihara (1978, 1986), but also numerical labels representing the number of surfaces in front of and behind the corresponding 3D edge. Labelling lines by their depth was first suggested by Huffmann (1971), one of the pioneers in this field.

We restrict our study to wireframe projections from a general viewpoint of objects with C^3 edges and surfaces meeting non-tangentially at trihedral vertices. This is a first step towards a more general scheme allowing objects with discontinuities of surface curvature (Cooper, 1993, 1997) or tetrahedral vertices (Varley and Martin, 2001). Figure 1(a) shows two drawings which can be shown to be physically unrealisable by semantic line labelling alone. In each case there would have to be an illegal label transition along the line AB. Figure 1(b) shows three drawings which require numerical depth labels as well as semantic labels to demonstrate their non-realisability. Although a consistent labelling exists in terms of semantic labels alone, they are clearly spatially incoherent.

If the drawing contains linear features such as straight lines, parallel lines or colinear lines, then further constraints can be deduced concerning the 3D positions of object vertices. These constraints give rise to linear equations or linear inequalities between the depths z_i of object vertices (in the case of orthographic projection) or between the inverses $t_i = 1/z_i$ of these depths (in the case of perspective projection) (Cooper, 2000). In a standard technique, pioneered by Sugihara

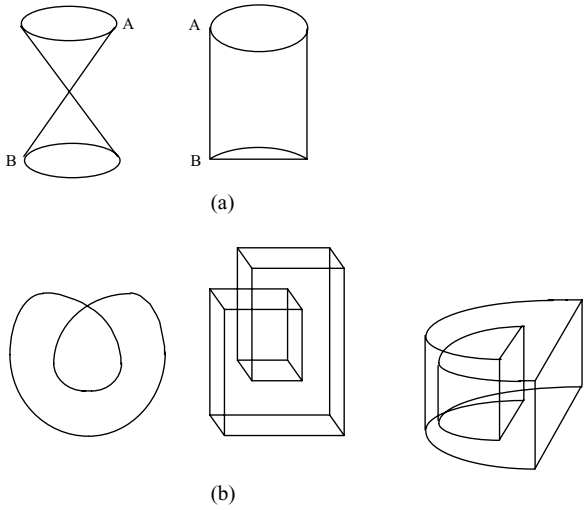

Figure 1. Examples of line drawings which do not have legal labellings.

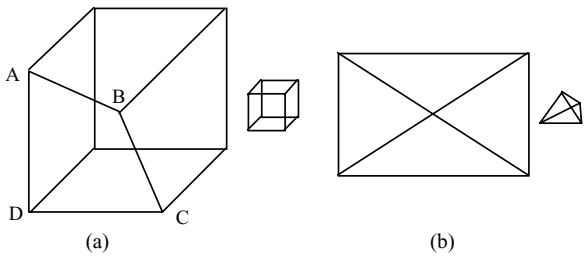

Figure 2. Two drawings which are impossible due to linear constraints.

(1986), the drawing is physically realisable if and only if the resulting linear programming problem has a solution.

Figure 2 shows two examples of drawings which have legal labellings (both semantic and numerical) but which are impossible by linear constraints. We assume a general viewpoint and orthographic projection, which imply that parallel lines in the drawing are projections of parallel lines in 3D. The existence of legal labellings follows from the fact that these drawings can be transformed into the drawings of a cube and a tetrahedron (shown in Fig. 2) by changes to positions of junctions which do not alter the configuration of the drawings. In Fig. 2(a), coplanarity constraints deduced from assumptions about the formation of straight edges imply that A, B, C, D are coplanar. However, using the constraint that parallel lines in the drawing are projections of parallel 3D edges, it is possible to deduce that B

does not lie in the same plane as A, D, C. As another example, the presence of parallel lines imples that the object represented in Fig. 2(b) is completely flat which contradicts the fact that all lines, including the two diagonals, are supposed to be projections of surface-normal discontinuities.

In the machine reconstruction of a 3D object model from a human-entered drawing, it is essential that the drawing be unambiguous. Wireframe models are often said to be ambiguous (see, for example, (Mortenson, 1997)) because they do not contain surface information (as in B_rep models) nor volume information (as in CSG models). However, we will show that wireframe models of polyhedra containing only simple trihedral vertices are, in fact, unambiguous.

2. Semantic and Numerical Line Labels

We make the following simplifying assumptions:

1. Objects are regular solids bounded by C^3 surfaces separated by C^3 edges (discontinuities of surface orientation).
2. Object vertices are trihedral, i.e. formed by the intersection of 3 surfaces. The edges and surfaces meeting at a vertex meet non-tangentially.
3. If the scene contains more than one object, then the objects are in general relative position: a small perturbation in their relative position does not alter the configuration of the drawing (such as the presence of junctions, straight lines or parallel lines).
4. The drawing is a projection of object edges (including viewpoint dependent edges such as the side of a cylinder) from a general viewpoint, i.e. a small perturbation in the viewpoint position does not alter the configuration of the drawing.

These assumptions exclude certain classes of interesting drawings, such as those involving objects with smooth edges or non-trihedral vertices. This preliminary paper presents basic results which we hope will serve as a foundation for later work on more complex objects.

Each line L joining two junctions in the drawing can be assigned

(a) a semantic label from the 6 possible labels $+$, $-$, $\leftarrow$, $\rightarrow$, $\Leftarrow$, $\Rightarrow$ according to the form of the 3D edge E projecting into L

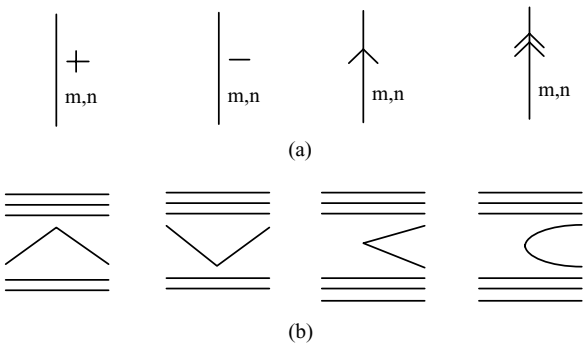

Figure 3. (a) The four distinct line labels; (b) cross-sections of the corresponding 3D edges.

(b) a pair of numerical labels m, n representing the number of surfaces m lying between the viewpoint and E, and the number of surfaces n lying behind E.

The meaning of the semantic labels $+$, $-$, $\rightarrow$, $\Rightarrow$ are demonstrated by their cross-sections shown in Fig. 3. In the example cross-sections of Fig. 3(b): $m = 3$ and $n = 2$ for the lines labelled '$+$' and '$-$'; $m = 3$ and $n = 3$ for the lines labelled '$\rightarrow$' and '$\Rightarrow$'. The label '$+$' means that the two surfaces meeting at E subtend an angle greater than π when observed from the viewpoint. The label '$-$' means that this angle is less than π.

We say that an edge E is visible if there is no surface lying betwen E and the viewpoint. An edge which is not visible is called hidden. A 3D edge E is called convex (concave) if the two object faces which intersect to form E subtend an angle less than π (greater than π) in the interior of the obejct. If a line L labelled '$+$' ('$-$') is the projection of a visible edge E then E is a convex (concave) edge. Note that this is not necessarily the case for hidden edges. In fact, the label $(+, m, n)$ represents a convex edge if m is even and a concave edge if m is odd. Similarly, the label $(-, m, n)$ represents a concave edge if m is even and a convex edge if m is odd.

The semantic label $\rightarrow$ means that the corresponding edge is the intersection of two object faces both of which project onto the right hand side of the line as we follow the direction of the arrow. The label $\rightarrow$ represents a surface-normal discontinuity, i.e. the intersection of two non-tangential object surfaces, whereas the label $\Rightarrow$ represents a viewpoint-dependent edge (extremal edge) which is the locus of points at which the line of sight is tangential to an object surface. Again the object surface projects onto the right hand side of the line as we follow the direction of the arrow. For

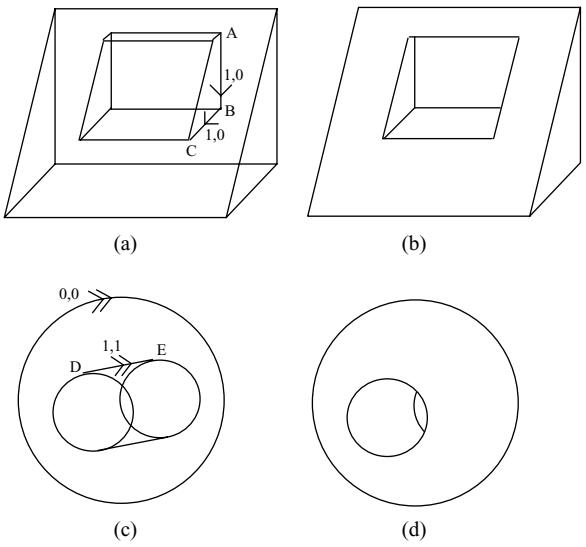

Figure 4. (a),(c) Two wireframe drawings of the 3D opaque objects illustrated in (b),(d), respectively.

example, a sphere projects into a circle labelled $\Rightarrow$. Note that, purely for typographical reasons, extremal edges are labelled by a double-headed arrow in the figures but by the symbol $\Rightarrow$ in the text of the paper.

Figures 4(a) and (c) show two wireframe drawings of objects with holes. Figures 4(b) and (d) are drawings of the corresponding 3D solid opaque objects in which only visible edges are shown. Note that the lines AB and BC in Fig. 4(a) and line DE in Fig. 4(c) all represent boundaries of holes and it is the hole which lies to the right of the line as we follow the direction of the arrow.

Figure 5 shows a simple wireframe projection with a legal labelling of each line segment. According to the labelling of Fig. 5, we can deduce that the 3D edge CD lies in front of the 3D edge AB. Note that the line AB in Fig. 5(b) is labelled '$-$' even though it is the projection

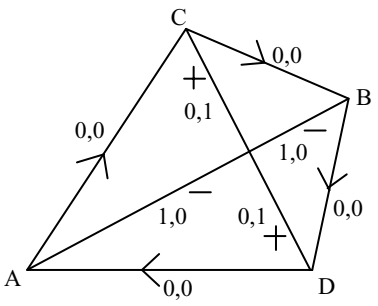

Figure 5. A simple wireframe projection labelled with both semantic and numerical labels.

of a convex 3D edge since its depth $m = 1$ is odd.

Junctions in a wireframe projection can be classified as follows. Let J be a junction at which three lines L_1, L_2, L_3 meet non-tangentially and let E_1, E_2, E_3 be the 3D edges which project into L_1, L_2, L_3. Assume that the lines are numbered so that the angles between L_1, L_2 and between L_2, L_3 are both less than π. If the angle between L_3, L_1 is greater than π, then J is a W junction, otherwise J is a Y junction. If E_1 lies behind the plane of E_2, E_3 then J is classified as a $W(+)$ or $Y(+)$ junction, otherwise a $W(-)$ or $Y(-)$ junction. When two lines cross they form an X junction. At 2-tangent and 3-tangent junctions, two or three lines meet tangentially.

Figure 6 shows a labelled wireframe projection involving curved lines. In this figure, junctions have been identified by their junction-type (2-tangent, 3-tangent, $W(+)$, $W(-)$, etc.). Although a labelled wireframe projection is still ambiguous, since we do not know the depth of any point on any object surface, the labels provide valuable local shape information at each edge and vertex as well as topological information concerning object faces.

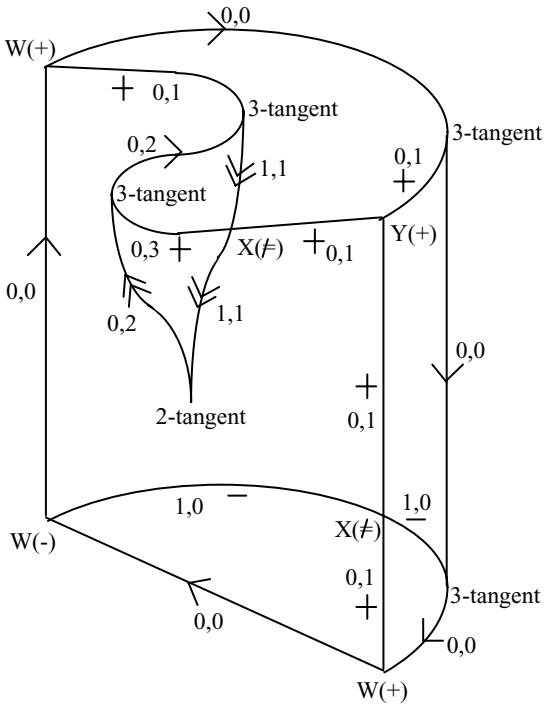

Figure 6. An example of a labelled wireframe projection.

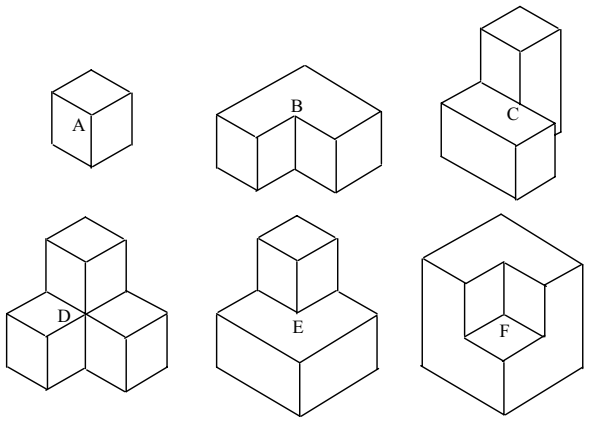

Figure 7. The six basic vertices formed by the intersection of three non-tangential surfaces.

3. Necessary and Sufficient Conditions for Realisability

When three surfaces meet non-tangentially at a point to form a 3D vertex, their tangents divide space into eight octants. Each octant may be empty or filled with matter. Figure 7 shows the six possible trihedral vertices thus obtained by this classic technique (Clowes, 1971; Huffman, 1971). (There is, in fact, a seventh vertex which is not shown since it is simply a reflected version of the vertex C). The viewpoint may be situated in any of the eight octants, including those filled with matter. By exhaustion, we obtained the list of all semantically and numerically labelled projections of the vertices in Fig. 7 from all possible viewpoints. For example, the vertex B in Fig. 7 projects into the 8 labelled junctions of Fig. 8(a). To obtain the numerical labels, we assume that any number of object surfaces can lie in front of or behind the vertex. Thus the numbers m, n are arbitrary non-negative integers. A physical realisation of each of these 8 labellings is shown in the wireframe projection of a holed cube shown in Fig. 8(b). The complete catalogue of labelled junctions representing projections of trihedral vertices is given in Figs. 9 and 10 under the headings $W(+)$, $W(-)$, $Y(+)$, $Y(-)$, $X(=)$, snowflake.

Even if the drawing contains only a single object, one edge may pass in front of another without intersecting it in 3D space. The resulting junction is known as an $X(\neq)$

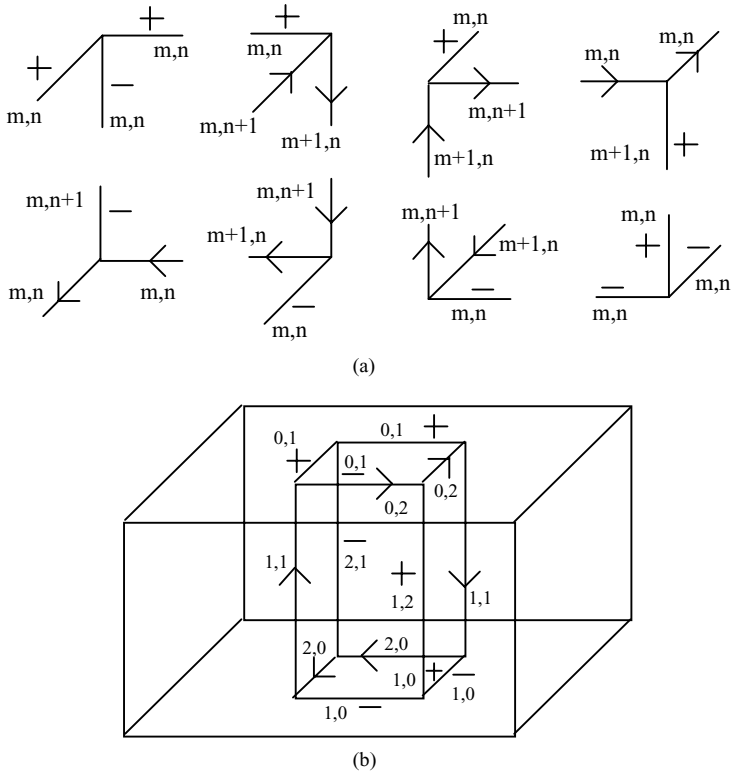

Figure 8. (a) The labelled junctions which can occur in a wireframe projection of vertex B in Fig. 7; (b) a wireframe projection demonstrating the physical realisability of each the these labellings.

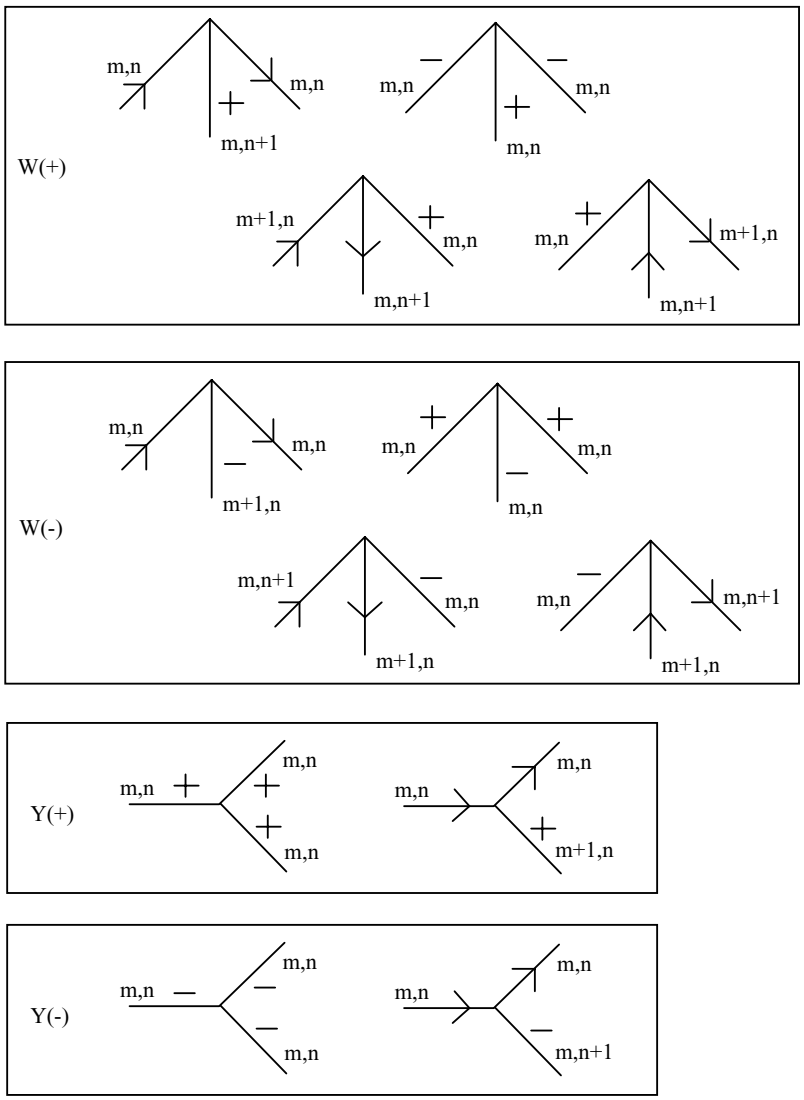

Figure 9. Catalogue of labelled W and Y junctions in wireframe projections.

junction (as opposed to an $X(=)$ junction which is the projection of a vertex at which two edges intersect, such as vertex C in Fig. 7). An example of an $X(\neq)$ junction is shown in Fig. 6. We call the projection of vertex D in Fig. 7 a snowflake junction. Note that certain workers have chosen not to include the vertices which project into $X(=)$ and snowflake junctions in the list of possible vertices.

The distinction between $W(+)$ and $W(-)$ junctions and between $Y(+)$ and $Y(-)$ junctions was first made by Parodi and Torre (1994). We can classify, for example, a W junction as $W(+)$ or $W(-)$ if we have information about the relative directions of the corresponding 3D edges, obtained from vanishing points. If such information is not available, then the set of labellings for a W junction is simply the union of the sets of labellings for $W(+)$ and $W(-)$ junctions. Purely for compactness of presentation, we have omitted from the list of legal labellings for Y, X and snowflake junctions those labellings which can be obtained by a simple rotation of those given in Figs. 9 and 10. After incorporating these rotated versions, a $Y(+)$ junction, for example, has exactly the same number of labellings as a $W(+)$ junction.

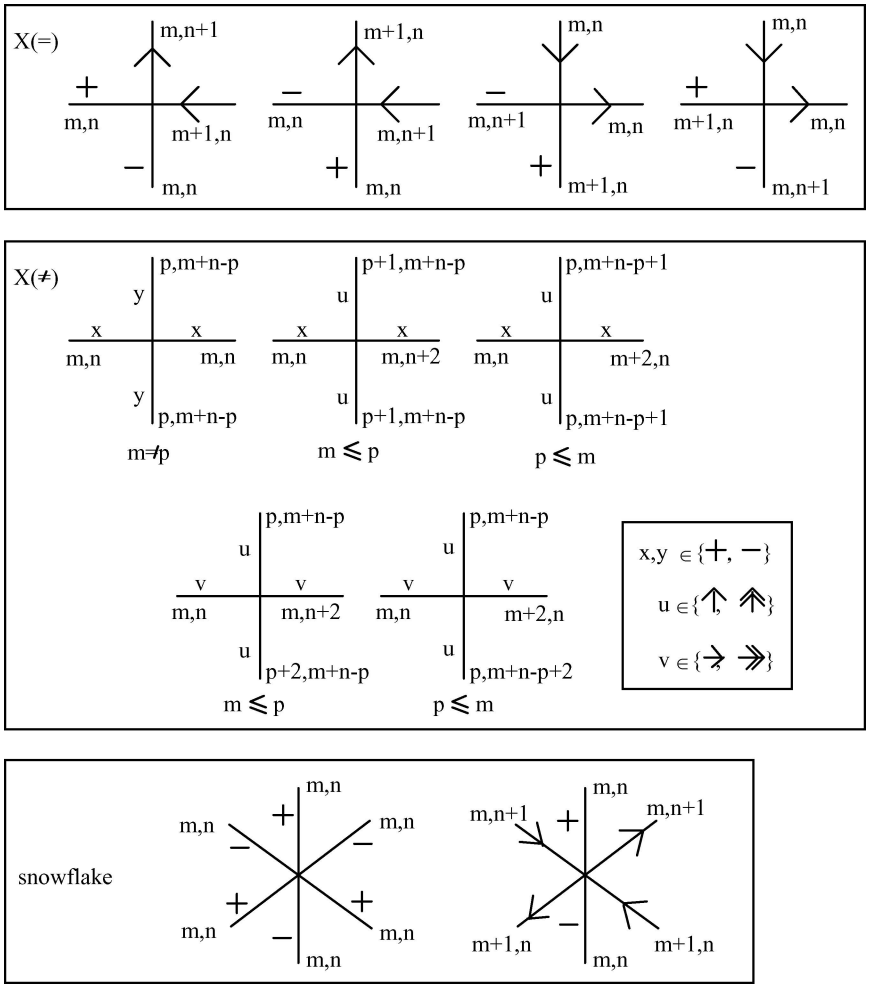

Figure 10. Catalogue of labelled X and snowflake junctions in wireframe projections.

Finally, curved surfaces give rise to viewpoint-dependent junctions involving projections of extremal edges. Examples of the resulting types of junction, known as 2-tangent and 3-tangent, are illustrated in Fig. 6. The legal labellings of 2-tangent and 3-tangent junctions are listed in Fig. 11. At a 3-tangent junction J, two of the lines meeting at the junction form a C^3 curve L which passes through J, whereas the third line L' terminates at J and exhibits a discontinuity of curvature with L. The line L' is shown as a horizontal straight line in Fig. 11, but may be curved (Cooper, 1993; Malik, 1987). Again purely for compactness of presentation, we have also omitted a reflected version of the 3-tangent junction in which the line L' goes off to the right instead of to the left.

In the catalogue of labelled junctions in Figs. 9–11, the numbers m and n are non-negative integers. A further unary constraint exists on each line label (s, m, n). This unary constraint, which follows directly from the reasonable assumption that the viewpoint lies outside all objects and that no object is of infinite extent, can be stated as follows:

Parity constraint:

if $s =$ ‘ $+$ ’ or ‘ $-$ ’ then $m + n$ is odd;

if $s =$ ‘ $\rightarrow$ ’ or ‘ $\Rightarrow$ ’ then $m + n$ is even.

If we assume that the wireframe projection is a projection of the whole 3D scene, in the sense that all 3D edges and surfaces are completely visible and not clipped by the picture boundary, then we have the following stronger constraint.

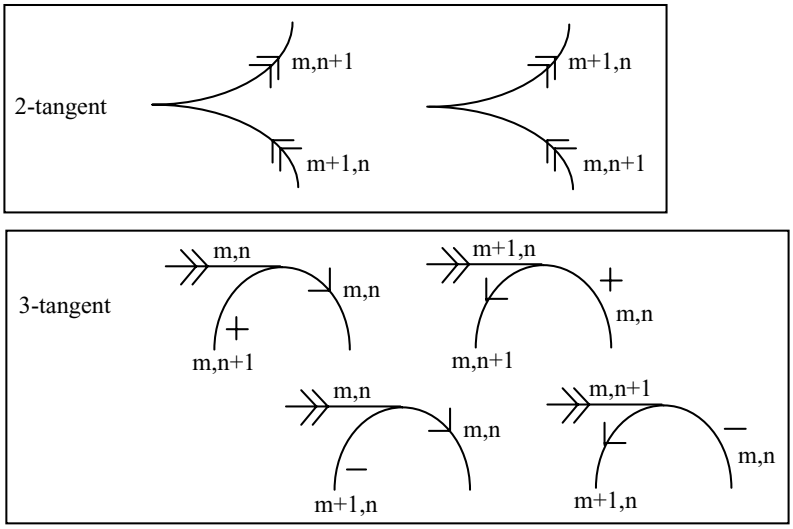

Figure 11. Catalogue of labelled 2-tangent and 3-tangent junctions in wireframe projections.

Outer boundary constraint:

all lines on the outer boundary of the wireframe projection are labelled $(\uparrow, 0, 0)$ or $(\Uparrow, 0, 0)$, since they correspond to occluding edges of objects.

As an example of the strength of these constraints, consider the wireframe projection in Fig. 12. Its boundary has been labelled in accordance with the Outer Boundary Constraint. From the list of labellings for W junctions, we see that each of the lines AD, BE, CF must have label $(+, 0, 1)$ or $(-, 1, 0)$, and hence two of these lines must have the same label. Without loss of generality, suppose that lines AD and BE are both labelled $(+, 0, 1)$. But then the labelling of junction X is illegal according to the catalogue of Fig. 10. Similarly, each of the wireframe projections in Fig. 1

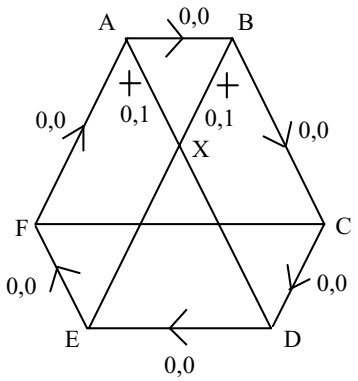

Figure 12. An example of an impossible wireframe projection.

are physically impossible, since none of them have a semantic and numerical labelling satisfying the above constraints.

There is also another constraint which is necessary when a wireframe projection can be decomposed into several connected components. To state this new constraint, we require the following definition.

Definition 3.1. In a wireframe projection (considered as a planar graph G), let R be a connected region (i.e. face of G) containing holes $H_1, \ldots, H_g$ (i.e. connected components of G entirely surrounded by R). The *frontier* of R is defined as the list of line segments forming the outer perimeter of R (visited in clockwise order) together with the lists of line segments forming the perimeters of $H_1, \ldots, H_g$ (each visited in anticlockwise order).

Region constraint:

if line segments L_1, L_2 form part of the frontier of the same connected region R, then $f_R(L_1) = f_R(L_2)$, where $f_R(L)$ is the number of surfaces projecting into the region to the right of the line L and is given by:

$f_R(L) = m + n + 1$ if L is labelled $(+, m, n)$ or $(-, m, n)$;
$f_R(L) = m + n + 2$ if L is labelled $(\uparrow, m, n)$ or $(\Uparrow, m, n)$;
$f_R(L) = m + n$ if L is labelled $(\downarrow, m, n)$ or $(\Downarrow, m, n)$.

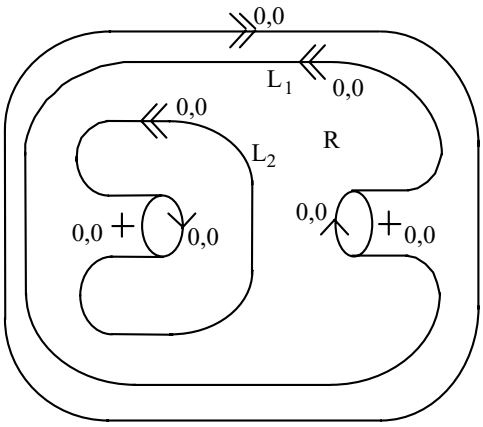

Figure 13. An impossible wireframe projection. For example, the labelling shown violates the region constraint on lines L_1, L_2 of region R.

Note that the region constraint is redundant if L_1, L_2 belong to the same connected component of the wireframe projection. This is because, by construction of our catalogue from projections of physically realisable vertices, the region constraint holds for lines L_1, L_2 meeting at a junction (and forming part of the frontier of the same region) and hence, by induction, for such lines L_1, L_2 joined by a sequence of junctions. Nevertheless, the region constraint is essential. Figure 13 shows an example of an impossible wireframe projection whose impossibility would not be detected if the region constraint were not applied.

Note that it can easily be shown that the parity constraint is redundant if the outer boundary and the region constraints are both applied.

Definition 3.2. A labelling of a wireframe projection is *legal* if each junction labelling occurs in the catalogue of Figs. 9–11 and the outer-boundary and region constraints are also satisfied.

Theorem 3.3. *A line drawing of curved objects is realisable as the wireframe projection of a* 3*D scene satisfying the conditions* 1, 2, 3, 4 (*given in Section* 2) *if and only if it has a legal labelling.*

Proof: The catalogue was constructed by listing all types of 3D vertices allowed by conditions 1, 2, 3, 4 and studying all possible projections from different viewpoints. It follows immediately that each junction in a wireframe projection must have a labelling in the catalogue. This shows that the catalogue represents a necessary condition for realisability. Similarly, the necessity of the outer-boundary and region constraints have also been shown above.

To show that the existence of a legal labelling is a sufficient condition for realisability, note firstly that all labellings have been included in the catalogue because they are projections of allowed vertices. Therefore, taken separately, all labelled junctions are realisable as projections of 3D vertices satisfying conditions 1, 2, 3, 4. It remains to show that we can join these vertices together to form a 3D object.

Consider the drawing as a partition of the plane into non-intersecting regions. For each region A, calculate n the number of surfaces which project into A. This number is well-defined by the region constraint. Lay n rubber sheets of the same 2D shape as A on top of each other and on the region A in the drawing. For each line segment L in the drawing, create a convex, concave, occluding or extremal edge according to the semantic label s of L at the depth given by the numerical label m, n of L as follows: if s is '+' or '−' then this means creating a convexity or concavity in the rubber sheet which lies at depth $m + 1$; if s is '↑' or '⇑' then this means joining the rubber sheets lying at depths $m + 1$ and $m + 2$ in the region to the right of L to create either a surface-normal discontinuity edge or an extremal edge. The rubber sheets partition 3D space into non-overlapping subsets. It only remains to specify which subsets should be filled with matter and which left empty. For any region R of the drawing, there will be matter between sheets at depth $m = 2i$ and $m = 2i + 1$ (for all i). The parity constraint ensures that the resulting 3D scene constructed from a wireframe projection will be of finite depth. □

Theorem 3.3 not only generalises Sugihara's groundbreaking work (Sugihara, 1978) to curved objects, but we have also considerably simplified the expression of his original constraints. As an example of the use of Theorem 3.3, consider the wireframe projection of Fig. 14(a) (adapted from an example given by Ernst (1986)). The given labelling is legal and hence this is a physically realisable wireframe projection. The corresponding opaque object is shown in Fig. 14(b) and a method of constructing it from a flexible tube with triangular cross-section is shown in Fig. 14(c).

4. All Wireframes are Ambiguous

It is well-known that wireframe projections can be ambiguous (Markowsky and Wesley, 1980; Mortenson,

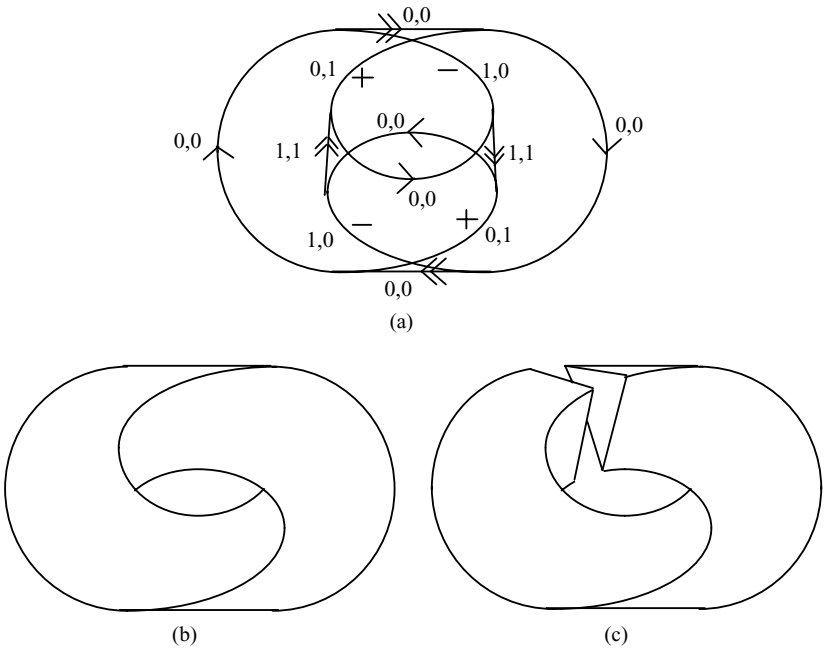

Figure 14. (a) *A* legally labelled wireframe projection, (b) the corresponding opaque object, (c) how to construct the object.

1997). In this section we prove a negative result concerning the ubiquity of ambiguity, which will help us to put into perspective the positive results of later sections.

Theorem 4.1 (*Depth Reversal Theorem*)**.** *Consider a legal labelling of a wireframe projection P. If we have no depth information (such as the identification of a W junction as a $W(+)$ or a $W(-)$ junction), then another legal labelling of P can be obtained by the following depth-reversal operation*: (1) *change all '$+$' labels to '$-$' and vice-versa*, (2) *change all numerical labels m, n to n, m.*

Proof: The proof is trivial by exhaustion over all labellings in the catalogue. For example, the first labelling for the $W(+)$ junction in Fig. 9 is transformed into the first labelling for the $W(-)$ junction by the above operation. It is trivial to check that the outer-boundary and region constraints cannot be invalidated by the depth-reversal operation. □

When the object represented by the wireframe projection is a cube, then this result corresponds to the famous Necker cube ambiguity. Interestingly, no junction labelling in our catalogue can be transformed into itself by the depth-reversal operation. This leads to the following result.

Lemma 4.2. *The only physically possible wireframe projections which are not subject to a depth-reversal ambiguity are those involving no junctions and in which all lines are labelled '$\rightarrow$' or '$\Rightarrow$'.*

Theorem 4.3. *All physically possible wireframe projections are ambiguous.*

Proof: Lemma 4.2 tells us that the only case to consider is when the wireframe projection contains no junctions. But in this case any curve C may be labelled '$\rightarrow$' or '$\Rightarrow$'. For example, a circle may be the projection of a sphere or a disk-shaped object. □

Imagine a drawing consisting of n mutually intersecting circles. There are at least $2^n n!$ interpretations of the drawing as a wireframe projection of a 3D scene, since each circle could be the projection of either a sphere or a disk and there are $n!$ possible depth orderings of the n objects.

There is another form of systematic ambiguity in wireframe projections which we call matter/space ambiguity. This occurs when it cannot be determined whether a subset of 3D space bounded by a set of surfaces represents an object or a hole. For example, in a wireframe projection consisting of just two concentric circles, the inner circle could represent a sphere in front of or behind another larger sphere, or could represent a hole inside an outer sphere.

5. Identifying Faces

An essential part of the interpretation of a wireframe projection is the identification of object faces. First of all we require a formal definition of a face.

From our assumptions on object shape in Section 2, a 3D edge E is the intersection of two 3D surfaces with distinct surface normals at every point of E. Each edge has a direction. As we walk along E in this direction and on the exterior of the object, let $S_L(E)$ represent the surface on our left and $S_R(E)$ the surface on our right.

Definition 5.1. Let $B = (E_1, \ldots, E_r)$ be a circuit of 3D edges such that, for $i = 1, \ldots, r$, V_i is the end-point of E_i and the start-point of E_{i+1} (where E_{r+1} is understood to mean E_1). Then B is a 3D *face-boundary* if, for $i = 1, \ldots, r$, E_{i+1} is the first edge leaving V_i which lies to the right of E_i on $S_R(E_i)$.

By this definition, $S_R(E_i) = S_R(E_{i+1})$ at each V_i and hence B is a boundary of the face which lies to its right.

Definition 5.2. *A face* of a 3D object is a closed connected C^3 surface patch P bounded by non-intersecting 3D face-boundaries $B_1, \ldots, B_h$ for some $h \geq 0$.

If the face is planar, then one of $B_1, \ldots, B_h$ is the outer boundary and the others are boundaries of holes. For curved surfaces, no such distinction can be made. For example, the curved surface of a cylinder has two circular 3D face-boundaries, neither of which is the outer boundary. A sphere has a single face with no 3D face-boundary (i.e. $h = 0$ in Definition 5.2). Note that a face may touch itself at a point (as does surface S_1 in Fig. 15(a)) or along an edge (as does surface S_4 in Fig. 15(b)). According to Definition 5.2, the surfaces S_2 and S_3 of Fig. 15(a) cannot be merged to constitute a single face. Furthermore, the 3D face-boundary of S_1 is necessarily (a, b, c, d, e, f, g, h, i, j); it is not possible to interpret (e, f, g, h) as a hole boundary and (a, b, c, d, i, j) as an outer boundary.

Definition 5.3. *A face-circuit* in a wireframe projection is a circuit of line segments which are the projection of the 3D face-boundary of an object face.

The identification of face-circuits is a major step in converting a wireframe model into a surface-based model such as a B_rep (Lipson and Shpitalni, 1996; Shpitalni and Lipson, 1996; Vosniakos, 1997, 1998). In fact, we will show that face-circuits can be unambiguously deduced from the labelling of a wireframe projection.

Each labelled junction in Figs. 9–11 is the projection of a 3D vertex. (In fact, each labelled junction corresponds to two distinct vertices, due to the matter/space ambiguity, but such ambiguity does not affect face-circuits.) By reconstructing a 3D vertex projecting into each labelled junction, we deduced the face-circuit information given in Figs. 16–18. In these figures, thick lines represent lines present in the wireframe projection, whereas thin lines represent fragments of face-circuits. The face-circuit line drawn on the left (right) of a line L labelled '+' or '−' corresponds to the face projecting into the region to the left (right) of L. For a line labelled '↑', the two face-circuit lines are both drawn to the right of L: the face-circuit line which is nearer to (farther from) L corresponds to the face which is nearer to (farther from) the viewpoint.

For brevity of presentation, $X(\neq)$ junctions are not given in Fig. 17. The presence of a $X(\neq)$ junction on

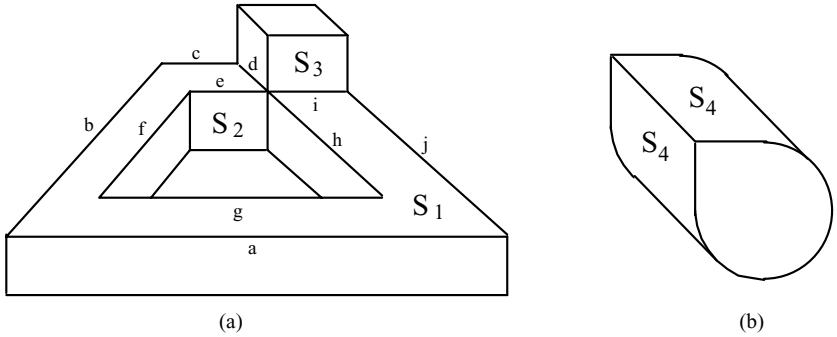

Figure 15. S_1, S_2, S_3, S_4 are examples of faces.

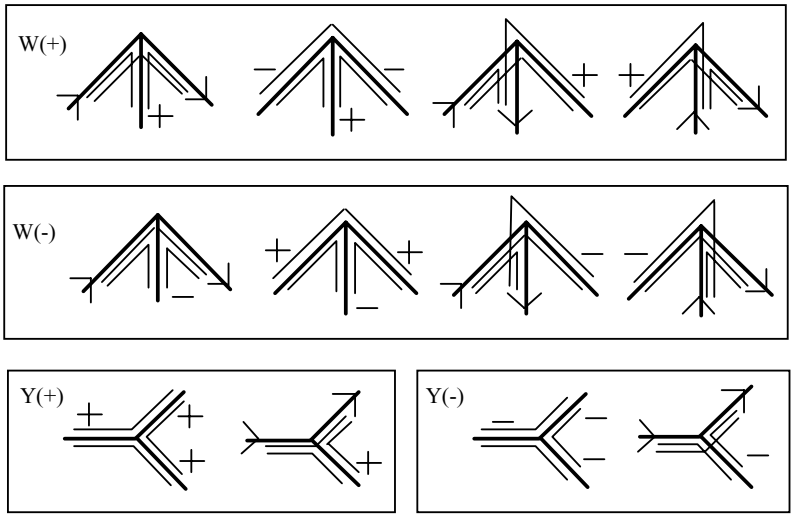

Figure 16. Catalogue of *W* and *Y* junctions with face-circuit fragments.

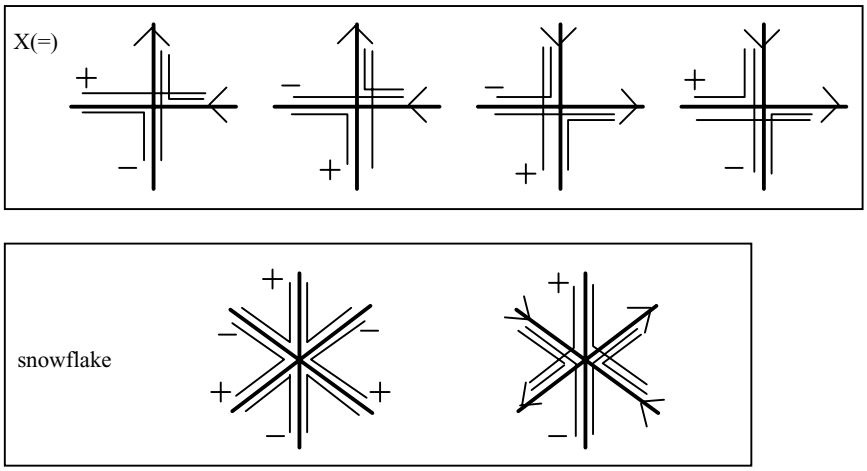

Figure 17. Catalogue of *X* and snowflake junctions with face-circuit fragments.

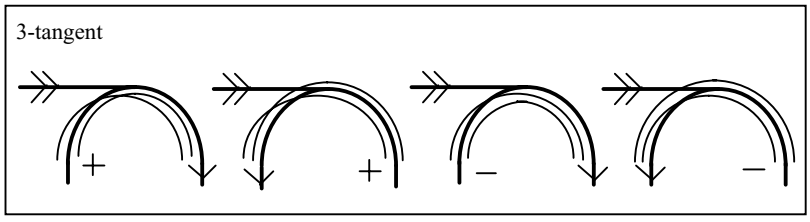

Figure 18. Catalogue of 3-tangent junctions with face-circuit fragments.

a line L has no effect on the face-circuit lines of L. Note that since extremal lines (i.e. lines labelled $\Uparrow$) are not projections of 3D edges, they do not belong to any face-circuit. This explains why we don't need to include 2-tangent junctions in Fig. 18. For clarity of presentation, the numerical labels are not shown on the lines in Figs. 16–18 but can be read off directly from the corresponding labelled junction in Figs. 9–11.

Theorem 5.4. *Given a legal labelling of a wireframe projection, we can uniquely determine the face-circuits of the corresponding 3D scene in linear time.*

Proof: Denote the wireframe projection by P. Each junction in a legal labelling of P uniquely determines face-circuit fragments, as illustrated by Figs. 16–18. It is then possible to determine complete face-circuits by concatenating these fragments. There is no possible ambiguity in the face-circuits in the construction. In the case of curved objects, Theorem 3.3 guarantees that a 3D scene exists which projects into P. □

Figure 19 shows an example of the determination of face-circuits of a wireframe projection. The wireframe projection in Fig. 19(a) has only two legal labellings. One legal labelling is shown in Fig. 19(a) and the other is its depth-reversal. For clarity of presentation, the numerical labels have been omitted (although they are essential in eliminating certain physically impossible labellings). Using the face-circuit constraints given in Figs. 16–18, we easily obtain the face-circuits shown in Fig. 19(b).

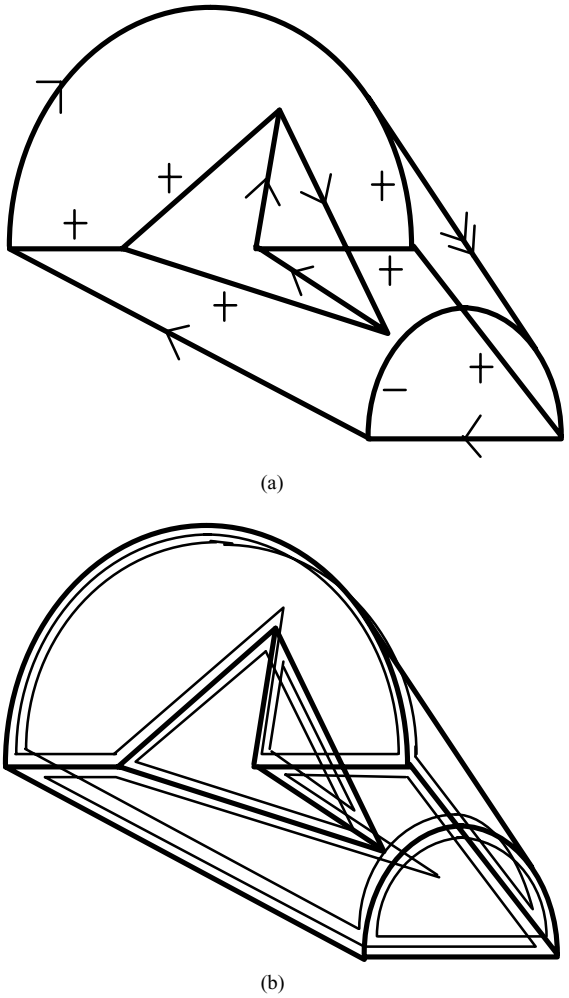

(a)

(b)

Figure 19. (a) A legally labelled wireframe projection; (b) its face-circuits derived from the catalogue of Figs. 16–18.

As another example, consider again the wireframe projection of Fig. 14(a). From the legal labelling given in the figure, the catalogue of Fig. 18 allows us to deduce that the corresponding object has just two 3D face-boundaries. In fact, as can be seen in Fig. 14(c), this object has a single face and is a version of the Möbius strip with a triangular cross-section.

Our approach consists in finding all possible semantic and numerical labellings of a wireframe projection (of which there may be an exponential number) and then determining the face-circuits for each such legal labelling. This can be compared with the traditional face-based approach (Markowsky and Wesley, 1980; Shpitalni and Lipson, 1996; Vosniakos, 1997, 1998). For example, Shpitalni and Lipson (1996) determine a set of possible face-circuits and then find maximal consistent sets of face-circuits. Their algorithm has worst-case time complexity which is exponential in the number of putative face-circuits, which is itself a potentially exponential function of the size of the drawing. We have thus reduced a doubly exponential complexity to a simple exponential complexity.

However, Definition 5.2 tells us that the projection of a face is, in fact, a set of face-circuits. In order to identify projections of faces, rather than just face-circuits, we use the same construction as in the proof of Theorem 3.3. Suppose we are given a legally labelled wireframe projection with regions $R_1, \ldots, R_t$. For each region R_i, we can easily determine the total number of faces $f(R_i)$ projecting into R_i. We can then, for each R_i, create f(R_i) copies $R_{i,1}$, $R_{i,2}$, ... of R_i which we call patches. To group together patches belonging to the same face it suffices to apply the following rule until convergence: patches $R_{i,u}$, $R_{j,v}$ are merged whenever (1) R_i, R_j are adjacent regions separated by a line L with numerical label (m, n) and $u = v \leq m$ or $f(R_i) - u = f(R_j) - v < n$ (i.e. $R_{i,u}$, $R_{j,v}$ correspond to the same face which either passes in front of or behind the 3D edge projecting into L), or (2) $i = j$, $u = m + 1$, $v = m + 2$ where the region R_i has a line L with label $(\Rightarrow, m, n)$ on its boundary (with R_i to the right of L as we follow the direction of the $\Rightarrow$ arrow).

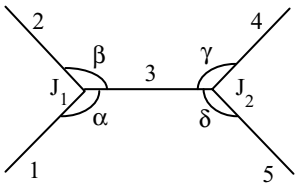

Figure 20. *A* generic W/Y junction pair (J_1, J_2). Note that lines 1–5 may be curved and the angles α, β, γ, δ may also be acute or reflex.

Each patch $R_{i,u}$ is a subset of a face (the projection of a face into region R_i). The set of patches thus represents an oversegmentation of the 3D object surfaces. Two adjacent patches seperated by a line L can be merged if L is the projection of a 3D edge lying on neither of the patches (case (1) above). Two patches can also be merged if they correspond to the same 3D face which folds over itself to form an extremal edge (case (2)).

6. Common-Surface Constraints

Instead of calculating face-circuits from legal labellings, it is sometimes possible to deduce face-circuit information directly without exhausting over all legal labellings. We will show in this section that face-circuit fragments can be directly determined given information concerning pairs of adjacent junctions. This information may be obtained, for example, from vanishing points or by applying local consistency operations to the labelling constraints of Section 3.

Remember that W and Y junctions can be classified as $+$ or $-$ depending on the relative 3D orientations of the edges which meet at the vertex which projects into the junction J. Knowledge of the vanishing points of the three lines which meet at J is sufficient to classify J as $+$ or $-$ (Parodi and Torre, 1994; Cooper, 2000). The following theorem tells us that knowing whether two W/Y junctions joined by a line are classified as the same or opposite sign allows us to determine two distinct triples of consecutive lines in face-circuits.

Consider a pair of junctions (J_1, J_2) joined by a line, where each of J_1, J_2 is either a W or a Y, as illustrated in Fig. 20. We call this a *W/Y junction pair*. Each of the lines 1-5 may be straight or curved and there may be any number of $X(\neq)$ or 3-tangent junctions on line 3 (but no $X(=)$ junctions). Let $n_{\text{refl}}(J_1, J_2)$ be the number of the angles α, β, γ, δ which are reflex (i.e. greater than π); let $n_{3t}(J_1, J_2)$ be the number of 3-tangent junctions lying on line 3; let $n_+(J_1, J_2)$ be the number of the junctions J_1, J_2 which are $+$ (i.e. $W(+)$ or $Y(+)$).

Theorem 6.1 (*Common-surface constraint*)**.** *Let (J_1, J_2) be a W/Y junction pair in a wireframe projection. If $p = (n_{\text{refl}}(J_1, J_2) + n_{3t}(J_1, J_2) + n_+(J_1, J_2))$ mod 2, then both $(1, 3, 5 - p)$ and $(2, 3, 4 + p)$ are triples of consecutive lines in a face-circuit, where line-numbers are as in Fig. 20.*

Proof: The result follows by simple exhaustion over all legal labellings of junction-pairs followed by reconstruction of the corresponding surfaces as in the proof of Theorem 5.4. □

It is important to note that, by our assumption that object edges are surface-normal discontinuities, we have implicitly disallowed a concave/convex transition on an edge. An example of such a transition is the point P in Fig. 21. In fact, the faces which intersect to form

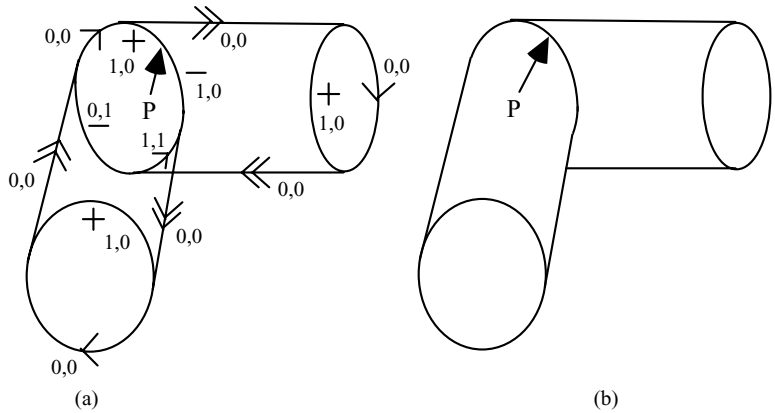

Figure 21. (a) A labelled wireframe projection involving a $+/-$ label transition at P; (b) a view of the corresponding opaque object.

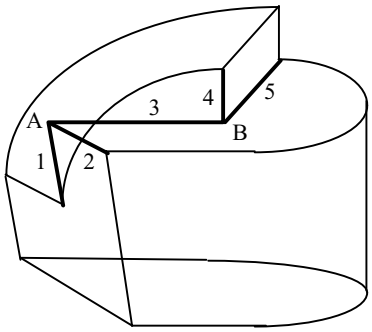

Figure 22. The coplanarity of lines 1, 3, 4 can be deduced despite the fact that they do not lie on the same face.

the edge are tangential at P (Cooper, 1997). Theorem 6.1 is no longer valid if $+/-$ transitions can occur on line 3 of Fig. 20.

7. Coplanarity Constraints

The presence of straight lines in a wireframe projection can provide information about the 3D positions of object vertices, provided we make the following assumption about object shape.

***Straight-edge formation assumption*:** any straight object edge is formed by the intersection of two locally planar surfaces.

This assumption was first stated in Cooper (2000) in the context of the interpretation of line drawings of opaque objects. It is clearly not always valid in man-made objects, but it allows us to extend techniques developed for polyhedral objects to a large class of curved objects. Under this assumption, neither 3-tangent junctions nor $+/-$ transitions (as in Fig. 21) can occur on straight lines. Most importantly, together with the general viewpoint assumption that we have already made, this new assumption means that straight lines in a wireframe projection can provide coplanarity constraints on edges. For example, the straight-edge formation constraint implies that if line-segments L_1, L_2, L_3 are consecutive line-segments in a face-circuit and L_1, L_2, L_3 are straight lines, then the 3D edges E_1, E_2, E_3 projecting into L_1, L_2, L_3 are coplanar. (Even if L_1 and L_3 are curved, we can still obtain a constraint, but this time involving the tangents to E_1 and E_3 at the vertices where they meet E_2. See Cooper (2000) for details.)

Thus Theorem 6.1 immediately provides coplanarity constraints provided that line 3 in Fig. 20 is a straight line. Note however, that we can say more: the coplanarity of a set of 3D edges may be detected even when the edges do not lie on the same face-circuit. Figure 22 shows an example. In this wireframe projection, knowing that A and B are both $W(+)$ junctions allows us to deduce that lines 1,3,4 are coplanar (as are lines 2,3,5). By exhausting over all cases, we discovered that the presence of any number of $X(=)$, $X(\neq)$ or snowflake junctions on line 3 in the W/Y junction-pair of Fig. 20 does not invalidate the coplanarity constraint, which we state formally as follows.

Theorem 7.1 (*Coplanarity constraint*)**.** *Suppose that lines* 1-5 *of the W/Y junction-pair* (J_1, J_2) *in Fig. 20 are straight lines and there are any number of X or snowflake junctions on line 3. If* $p = (n_{\text{refl}}(J_1, J_2) + n_+(J_1, J_2))$ *mod* 2, *then both* $(1, 3, 5\text{-}p)$ *and* $(2, 3, 4 + p)$ *are triples of coplanar lines.*

As an example of the strength of the coplanarity constraint, consider the wireframe projection shown in Fig. 23(a). The wireframe projection has two legal

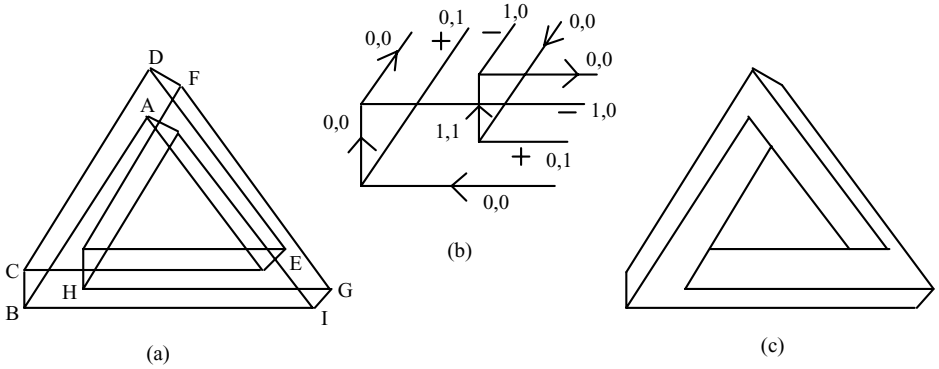

Figure 23. (a) a wireframe projection; (b) a part of a legal labelling; (c) the visible lines corresponding to this labelling.

labellings, one of which is the depth reversal of the other. The bottom left corner of one of these legal labellings is illustrated in Fig. 23(b). The visible lines of this labelling corresponds to the famous Penrose triangle (Penrose and Penrose, 1958) shown in Fig. 23(c). The physical impossibility of the wireframe projection follows from the coplanarity constraint. In both legal labellings, junction pairs B, C and C, D are both of opposite sign. It follows from Theorem 7.1 that both A, B, C, D and B, C, D, E are projections of sets of coplanar points. Hence A, B, C, D, E are projections of coplanar points. By symmetry, E, D, F, G, H are projections of coplanar points, as are H, G, I, B, A. These three planes should then meet at a point in 3D space, which implies that the lines AB, ED and HG, when extended, should meet at a point in the drawing. Since this is clearly not the case, the wireframe projection is physically impossible.

To obtain necessary and sufficient conditions for the realisability of a wireframe projection of curved objects involving straight lines, we require not only the coplanarity constraints deduced from Theorem 7.1, but also inequality constraints expressing the fact that the nearer line passes in front of the distant line at each $X(\neq)$ junction and that the two faces meeting at each concave (convex) edge subtend an angle less (greater) than π (Sugihara, 1986; Cooper, 2000). This leads to a linear programming problem P. However, a realisable wireframe projection may give rise to a problem P which has no solution due to rounding errors or small user errors in the positions of junctions. Different solutions have been proposed to overcome this problem of superstrictness (Sugihara, 1986; Ros and Thomas, 2002; Cooper, 2000). It should be noted that testing the realisability of a wireframe projection still involves solving a linear programming problem for each of a possibly exponential number of legal labellings.

8. Unambiguous Wireframes

Although all physically realisable wireframe projections are ambiguous by Theorem 4.3, we show in this section that the presence of extra information, together with some further restrictions on the class of 3D scenes, can eliminate all ambiguity either in the determination of the face-circuits or in the complete interpretation of the wireframe.

Definition 8.1. *A* vertex V is *simple* if none of the edges which meet at V continues through V.

Thus vertices which project into $X(=)$ or snowflake junctions are not simple.

Definition 8.2. *A* wireframe projection is *simple polyhedral* if it is a projection of a collection of polyhedral objects with simple vertices satisfying conditions 1, 2, 3, 4 (of Section 2).

Theorem 8.3. *Let P be a simple polyhedral wireframe projection. If for each W/Y junction pair (J_1, J_2), we know whether J_1, J_2 are of the same or of opposite signs, then the face-circuits of P can be unambiguously identified in linear time.*

Proof: Since P is simple polyhedral, it only contains junctions of type $W, Y, X(\neq)$. $X(\neq)$ junctions have no effect on face-circuits. The common-surface constraint of Theorem 6.1. allows us to construct without ambiguity the face-circuits of P. This can clearly be acheived in linear time, by extending face-circuit fragments until a closed circuit is obtained and restarting this procedure until each line is has been placed in two distinct face-circuits. □

Corollary 8.4. *Let P be a simple polyhedral wireframe projection. If for each line L in P, we know the position of the vanishing point of L, then the face-circuits of P can be unambiguously identified in linear time.*

Proof: By the assumption of a polyhedral scene, all edges are straight lines. The position of the vanishing point of each line L in P allows us to determine whether each W/Y vertex J of P is $+$ or $-$ (Parodi and Torre, 1994; Cooper, 2000). Thus, by Theorem 8.3, the face-circuits of P can be determined in linear time.

Sugihara (1978, 1986) and Alevizos (1991) both study a specific type of wireframe projection in which the user specifies, for each line L, whether L is of even or odd depth. In other words, if (m, n) represents the numerical label of L, the user must specify whether m is even or odd. We say that such a wireframe projection has depth-parity information.

Consider a W/Y junction pair as illustrated in Fig. 20. Recall that $n_{\text{refl}}(J_1, J_2)$ is the number of the angles $\alpha, \beta, \gamma, \delta$ in Fig. 20 which are greater than π. We say that a W/Y junction pair has even (odd) *angle-parity* if $n_{\text{refl}}(J_1, J_2)$ is even (odd). Given the depth-parity of each of the lines 1, 2, 4, 5 in a W/Y junction pair, we can also clearly determine the parity of the sum s of the depths of the lines 1, 2, 4, 5; we say that a W/Y

junction pair has even (odd) *depth-parity* if s is even (odd). Having established the necessary notation, we can now state the following lemma. □

Lemma 8.5. *Let* (J_1, J_2) *be a W/Y junction pair in a wireframe projection formed under assumptions* 1, 2, 3, 4 *of Section* 2. *If the angle-parity of* (J_1, J_2) *is the same as its depth-parity, then* J_1, J_2 *are of the same sign; otherwise* J_1, J_2 *are of opposite sign.*

Proof: The proof is simple, although tedious, by exhaustion over all possible labellings of all possible configurations of W/Y junction pairs. □

Thus, depth-parity information for each line allows us to deduce for each W/Y junction pair (J_1, J_2), whether J_1, J_2 are of the same or of opposite signs. Theorem 8.3 then provides us with a simple proof of the following result first stated by Alevizos (1991).

Corollary 8.6. *Let P be a simple polyhedral wireframe projection with depth-parity information. Then the face-circuits of P can be unambiguously identified in linear time.*

Under perspective projection, the vanishing points of all lines provide sufficient information to identify the sign of W/Y junctions. Under orthographic projection, on the other hand, the sign of W/Y junctions is inherently ambiguous, as illustrated by the depth-reversal phenomenon (see Section 4) in which all W/Y junctions change sign. However, we can use the fact that, under orthographic projection, if two lines L_1, L_2 in the wireframe projection are parallel then, by the general viewpoint assumption, L_1, L_2 are projections of parallel lines in 3D. If, in the generic W/Y junction pair shown in Fig. 20, all lines are straight lines and lines i and J are parallel (where $i \in \{1, 2\}$ and $j \in \{4, 5\}$), then it follows that lines i, 3, j are coplanar and hence, by the straight-edge formation assumption, that i, 3, j is a face-circuit fragment.

Corollary 8.7. *Let P be a simple polyhedral wireframe projection formed by orthographic projection. If all lines of P are parallel to one of only three directions, then the face-circuits of P can be uniquely determined in linear time.*

Proof: Since all lines of P are parallel to one of only three directions, at each W/Y junction pair there must be two pairs of parallel lines (either (1, 4), (2, 5) or (1, 5), (2, 4) where the numbers refer to the lines in Fig. 20). From the discussion above, at each W/Y junction pair, we can thus determine two face-circuit fragments (either (1, 3, 4), (2, 3, 5) or (1, 3, 5), (2, 3, 4)). The result then follows by the same argument as in the proof of Theorem 8.3. □

Theorem 8.8. *Let P be a simple polyhedral wireframe projection. If, for each vertex V in P, we know the 3D coordinates of the point which projects into V (i.e. we have a 3D wireframe model), then the semantic and numerical labelling of P is unique. Furthermore, the physical realisability of P can be checked and the semantic and numerical labelling of P can be found in quadratic time.*

Proof: From the 3D positions of vertices we can determine for each W/Y junction J in P whether J is $+$ or $-$. Theorem 8.3 then tells us that we can uniquely determine the face-circuits of P. Since we know the 3D coordinates of all vertices, we can then easily determine the 3D face-boundaries projecting into the face-circuits of P. In order to identify faces, it only remains to determine for each 3D face-boundary B, whether B is the outer boundary of a face or the boundary of a hole. Consider only those 3D face-boundaries $B_1, \ldots B_r$ which lie in the same plane Q_B as B. Let H_B be a half-line from a point on B to infinity within the plane Q_B such that H_B does not intersect any object vertex. Then B is an outer boundary (hole boundary) if the number of intersections of H_B with the 3D face-boundaries $B_1, \ldots B_r$ is even (odd). (Note that here we do not need to consider any intersections of H_B with faces which are not coplanar with B, which renders this operation much simpler than when it is performed as a means of identifying face-circuits (Jain, 1999; Markowsky and Wesley, 1980)).

For each line L in P, it is then trivial to determine the semantic label of L from the resulting set of faces. Furthermore, by tracing a ray R from the viewpoint through an arbitrary point on the 3D edge E_L which projects into L, and counting the number of faces which R intersects in front of and behind E_L, allows us to deduce the numerical label (m, n) of L.

To check the physical realisability of P we only need to determine for each pair of faces F_1, F_2, whether F_1, F_2 intersect. If they do, then this intersection must correspond to an edge on the 3D face-boundaries of both F_1 and F_2. □

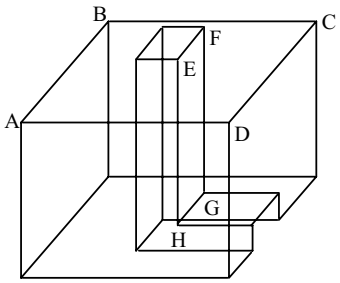

Figure 24. An example of an impossible 3D wireframe model of a polyhedral object.

As an example, Fig. 24 shows a physically impossible 3D wireframe model. It is illegal because the two faces *ABCD* and *EFGH* intersect along an edge whose projection is not present in the model. Note, on the other hand, that this wireframe model is physically realisable if the surface *ABCD* may be curved.

9. Discussion

It is worthwhile studying wireframe projections in which the assumptions of the uniqueness theorems of Section 8 have been relaxed, in order to see which kinds of ambiguity can occur. The simple polyhedral wireframe projection to the left of Fig. 25(a) is a perspective projection of a pair of cubes. Purely for illustrative purposes, certain lines have been drawn thicker than others, but no such distinction is actually present in the wireframe projection. We assume that the position of the three vanishing points (not shown in the figure) is known. By Corollary 8.4, all face circuits can be uniquely determined. However, we cannot determine whether one cube lies in front of, behind or inside the other. Thus the numerical labelling of lines is not unique. Furthermore, neither the semantic labelling nor the faces are unique, since if one cube lies inside the other then the bottom of the inner cube may be a face or a hole (as illustrated to the right of Fig. 25(a).

Under orthographic projection, the face-circuits of the wireframe projection shown to the left of Fig. 25(b) can be uniquely determined (by Corollary 8.7) provided $X(=)$ junctions cannot occur. This is despite depth-reversal ambiguity as well as relative depth ambiguity between the two objects. However, if $X(=)$ junctions may occur, then the wireframe projection may be interpreted as either of the two distinct cross-shaped objects

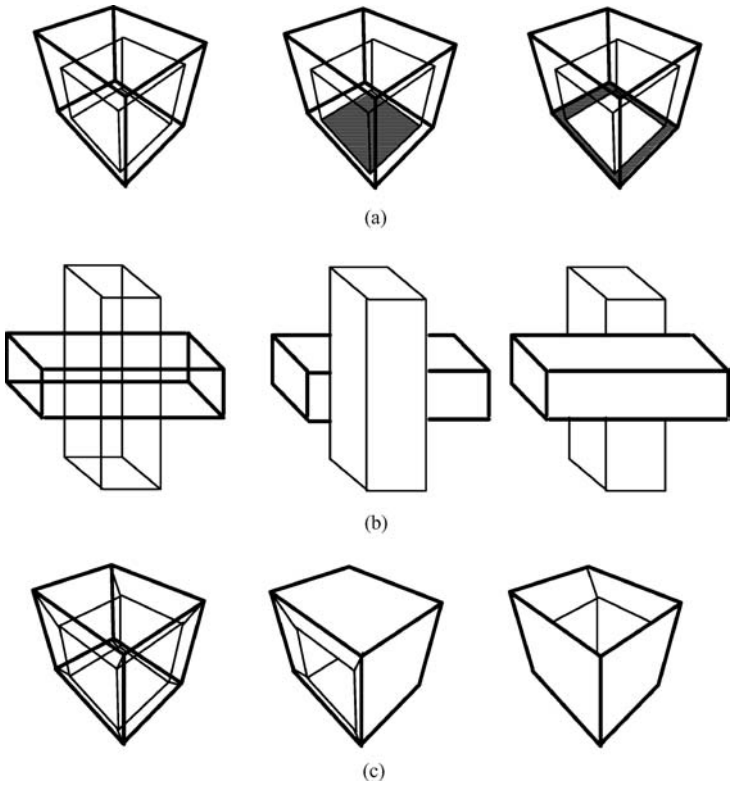

Figure 25. Examples of ambiguous wireframe projections.

(formed by sticking two rectangular objects together) shown to the right of Fig. 25(b). These two interpretations, as well as a third interpretation as two separate objects, all give rise to distinct sets of face-circuits.

Finally, the wireframe projection shown on the left of Fig. 25(c) is a classic example (Markowsky and Wesley, 1980; Mortenson, 1997) of an ambiguous 3D wireframe model with non-trihedral vertices. Two possible interpretations are shown to the right of Fig. 25(c). These interpretations clearly do not have the same face-circuits.

The main source of ambiguity in wireframe projections remains the missing depth dimension. Different heuristics have been proposed to choose among different interpretations of a wireframe projection, favouring commonly occurring features of man-made objects such as planarity, symmetry, orthogonality, equality of angles or lengths (Marill, 1991; Leclerc and Fischler, 1992; Lipson and Shpitalni, 1996). Leclerc and Fischler (1992) state an interesting condition for evaluating the psychological plausibility of a reconstructed object O, namely that the same object O be produced by the recovery algorithm from a wireframe projection of O from a different viewpoint.

10. Conclusion

A wireframe projection provides a convenient means of representing a 3D object from a single view. However, it is well-known that, even given complete depth information about lines, a wireframe model of a polyhedron is ambiguous. We have shown, however, that a 3D wireframe model of a polyhedron with simple trihedral vertices is unambiguous.

When a wireframe projection is human-entered, it is important to test its physical realisability. In the case of curved objects, we have given necessary and sufficient conditions for the physical realisability of a wireframe projection. These conditions are based on a novel labelling scheme involving the number of surfaces in front of and the number of surfaces behind each edge. When the wireframe projection contains linear features this leads to further constraints. Each straight line gives rise to a coplanarity constraint between object vertices.

Further research is necessary to extend the catalogue of labelled junctions to non-trihedral vertices (Varley and Martin, 2001), vertices at which surfaces or edges meet tangentially (Cooper, 1997) and non-manifold objects. Another possible extension of the labelling scheme would be to allow extra lines representing discontinuities of surface curvature, as has already been done for line drawings of opaque objects (Cooper, 1993, 1997).

References

Agarwal, S.C. and Waggenspack, W.N. Jr. 1992. Decomposition method for extracting face topologies from wireframe models. *Computer-Aided Design*, 24(3):123–140.

Alevizos, P.D. 1991. A linear algorithm for labeling planar projections of polyhedra. In *Proc. IEEE/RSJ International Workshop on Intelligent Robots and Systems IROS'91*, pp. 595–601.

Clowes, M.B. 1971. On seeing things. *Artificial Intelligence*, 2:79–116.

Cooper, M.C. 1993. Interpretation of line drawings of complex objects. *Image and Vision Computing*, 11(2):82–90.

Cooper, M.C. 1997. Interpreting line drawings of curved objects with tangential edges and surfaces. *Image and Vision Computing*, 15:263–276.

Cooper, M.C. 1999. Linear-time algorithms for testing the realisability of line drawings of curved objects. *Artificial Intelligence*, 108:31–67.

Cooper, M.C. 2000. Linear constraints for the interpretation of line drawings of curved objects. *Artificial Intelligence*, 119:235–258.

Cooper, M.C. 2001. The interpretation of line drawings with contrast failure and shadows. *International Journal of Computer Vision*, 43(2):75–97.

Ernst, B. 1986. *Adventures with Impossible Figures*. Tarquin Publications.

Huffman, D.A. 1971. Impossible objects as nonsense sentences. In *Machine Intelligence*, Melltzer, B. and Michie, D. (Eds.). Edinburgh University Press, Vol. 6, pp. 295–323.

Jain, P.K. 1999. Extraction of compound volumetric fatures from a three-dimensional wire frame model. *Procs of the Institute of Mechanical Engineers Part B Journal of Engineering Manufacture*, 213(6):597–613.

Kirousis, L.M. and Papadimitriou, C.H. 1988. The complexity of recognizing polyhedral scenes. *J. Comput. System Sci.*, 37(1):14–38.

Kuo, M.H. 1998. A Systematic Approach Towards Reconstructing 3D Curved Models from Multiple 2D Views. In *Graphics Recognition: Algorithms and systems; 2nd International Workshop, GREC'97*, K. Tombre and A.K. Chhabra (Eds.), LNCS 1389, Springer, pp. 265–279.

Leclerc, Y.G. and Fischler, M.A. 1992. An optimization-based approach to the interpretation of single line drawings as 3D wire frames. *International Journal of Computer Vision*, 9(2):113–136.

Lipson, H. and Shpitalni, M. 1996. Optimisation-based reconstruction of a 3D object from a single freehand line drawing. *Computer-Aided Design*, 28(8):651–663.

Malik, J. 1987. Interpreting line drawings of curved objects. *International Journal of Computer Vision*, 1:73–103.

Marill, T. 1991. Emulating the human interpretation of line- drawings as three-dimensional objects. *International Journal of Computer Vision*, 6(2):147–161.

Markowsky, G. and Wesley, M.A. 1980. Fleshing out wire frames. *IBM Journal of Research and Development*, 24(5):582–597.

Mortenson, M. 1997. *Geometric Modelling*. 2nd edn J. Wiley.

Parodi, P. and Torre, V. 1994. On the complexity of labeling perspective projections of polyhedral scenes. *Artificial Intelligence*, 70:239–276.

Penrose, L.S and Penrose, R. 1958. Impossible objects, a special kind of visual illusion. *British Journal of Psychology*.

Ros, L. and Thomas, F. 2002. Overcoming superstrictness in line drawing interpretation. *IEEE Trans. Pattern Analysis and Machine Intelligence*, 24(2).

Shpitalni, M. and Lipson, H. 1996. Identification of faces in a 2D line drawing projection of a wireframe object. *IEEE Trans. on Pattern Analysis and Machine Intelligence*, 18(10):1000–1012.

Sugihara, K. 1978. Picture language for skeletal polyhedra. *Computer Graphics Image Processing*, 8:382–405.

Sugihara, K. 1986. *Machine Interpretation of Line Drawings*. MIT Press: Cambridge, MA.

Syeda-Mahmood, T. 1999. Indexing of technical line drawing databases. *IEEE Trans. on Pattern Analysis and Machine Intelligence*, 21(8):737–751.

Varley, P.A.C. and Martin, R.R. 2001. The junction catalogue for labelling line drawings of polyhedra with tetrahedral vertices. *International Journal of Shape Modelling*, 7(1):23–44.

Vosniakos, G. 1997. Conversion of wireframe to ACIS solid models for $2^1/2$-D engineering components. *The International Journal of Advanced Manufacturing Technology*, 14(3):199–209.

Vosniakos, G. 1998. An intelligent software system for the automatic generation of NC programs from wireframe models of $2\text{-}^1/2$ D mechanical parts. *Computer Integrated Manufacturing Systems*, 11(1/2):53–65.

Wesley, M.A. and Markowsky, G. 1981. Fleshing out projections. *IBM Journal of Research and Development*, 25(6):934–954.